# Petrology and metallogeny associated with the Tryvann Granite Complex, Oslo Region

ODD NILSEN

Nilsen, O. 1992: Petrology and metallogeny associated with the Tryvann Granite Complex, Oslo Region. *Nor. geol. unders. Bull. 423,* 1-18.

The Tryvann Granite Complex (TGC) comprises four separate intrusive bodies within the Oslo Graben. It constitutes a differentiated suite of young (240 - 245 Ma) alkaline quartz syenites and granites derived from a strongly fractionated, hydrous residual melt which was emplaced during the collapse of the Bærum Cauldron. The emplacement occurred contemporaneously with the formation of the ring-dyke complex. Intramagmatic vein-type molybdenite, pyrite and Fe-oxide mineralizations occur associated with a widespread albitic hydrothermal alteration confined chiefly to fracture zones within the TGC complex. On a regional scale, the geological pattern, as revealed by gravimetric anomalies, and the spatial metamorphic and metasomatic alteration patterns adjacent to the southern part of the Bærum Cauldron, indicate the existence of a (partly) hidden, NE-SW trending, elongated plutonic complex to which the TGC may be related. This complex apparently follows a central volcanic axis which constitutes a possible plutonic link between the Bærum and Nittedal Cauldrons of the Oslo Graben.

*O. Nilsen, Institutt for Geologi, Universitetet i Oslo, 0316 Oslo 3, Norway.*

## Introduction

The Oslo Paleorift constitutes a well documented continental rift system of Permo-Carboniferous age. On land, the Oslo Rift forms a major graben structure — the Oslo Graben (Ramberg 1976) — which has been extensively studied for more than a century. Geophysical data have shown that the rift continues to the SSW into the Skagerrak sea, where it is bounded by Mid to Late Precambrian gneisses and migmatites (Ro et al. 1990). Comprehensive summaries of the Oslo Rift geology have been presented by Oftedahl (1960, 1980), Ramberg (1976), Dons & Larsen (1978), Neumann & Ramberg (1978) and Neumann (1990).

The Oslo Graben has been subdivided into two major graben segments, termed the Vestfold Graben (southern) and the Akershus Graben (northern). Within the graben the Precambrian basement is overlain by pre-rift Cambro-Silurian metasediments, which are folded in the central and northern part of the Oslo Region. They are inconformably overlain by a thin horizon of predominantly continental, Upper Carboniferous metasediments. However, Permian volcanites, metasediments and plutonic rocks make up the main lithologies of the Oslo Graben.

The Oslo Rift was magmatically active for more than 60 million years. Magmatism began at about 300 Ma (Late Carboniferous), and the rift went through several intrusive and volcanic periods up to about 240 Ma (Sundvoll et al.1990). The tectonomagmatic evolution of the Oslo Rift has been subdivided into different stages by Ramberg & Larsen (1978), Larsen & Sundvoll (1982) and Sundvoll et al. (1990). After initial fissure eruptions of plateau lavas of basaltic and intermediate, trachytic composition, a period of central volcano activity associated with cauldron collapses and ring-dyke formation took place. This central volcano stage seems to have continued into the main intrusive period with the emplacement of large batholiths of monzonite (larvikite), syenite and granite. The petrogenesis of these rocks has recently been extensively studied by Neumann (1978,1980,1988), Neumann et al.(1988) and Rasmussen et al.(1988).

Within the Oslo Graben magmatic rocks, chiefly of the alkaline kindred, cover more than 75% of the area. Along with the petrological and geochemical research, the metallogenetic aspects of hydrothermal, late- and post-magmatic processes associated with the magmatic activity have been investigated. Compre-

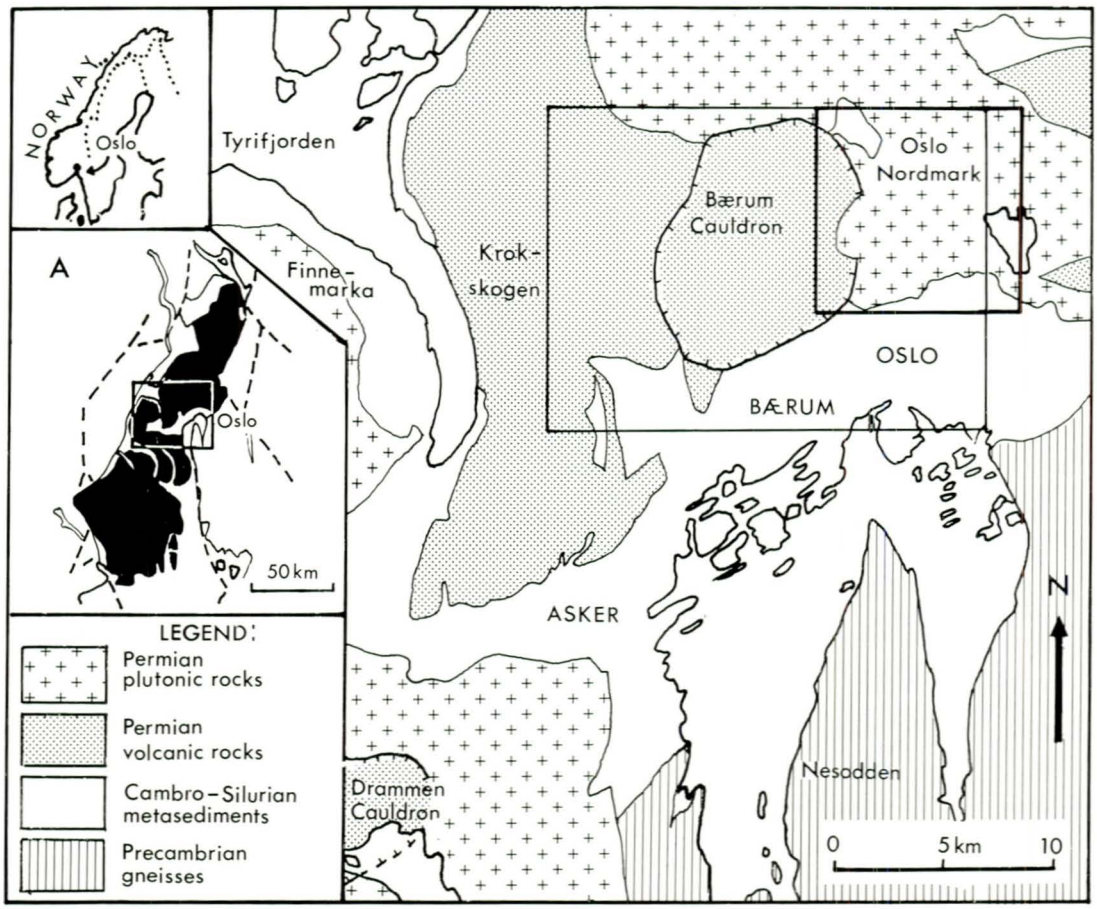


Fig. 1: Key map of the Oslo district with main geological elements. From Naterstad & Dons (1978). Inset map (A): The Oslo Rift with graben faults (stippled lines) and Permian igneous rocks (in black).

hensive accounts of the geological evolution and metallogeny of the Oslo Paleorift have recently been presented by Vokes (1973, 1988), Ihlen (1978,1986), Ihlen & Vokes (1978) and Bjørlykke et al.(1990), and intramagmatic and related exocontact deposits of molybdenite have been described as an important class of hydrothermal ore deposits in the Oslo Graben (Geyti & Schönwandt 1979, Ihlen et al.1982, Schönwandt & Petersen 1983, Pedersen 1986). The molybdenite deposits are related to highly differentiated extrusive and intrusive granitic rocks, temporally and spatially associated with the caldera formations and batholith emplacements during different stages in the tectonomagmatic evolution of the Oslo Rift.

Biotite granites are the major host for the intramagmatic Mo-deposits which include both vein- and stockwork-type mineralization. Based on their petrography and field and age relationships, the biotite granites (BG) of the Oslo Graben have been classified by Gaut (1981) into two major groups (BG1 and BG2). BG1 comprise the older (270-260 Ma) subsolvus granites which occur as large batholithic bodies emplaced during the early batholith stage (e.g. the Finnemarka and Drammen granites) (Fig.1). The BG2 granites are younger (250-240 Ma), hypersolvus alkali-feldspar granites which in general form smaller, stock-like bodies. They probably evolved as late-stage differentiation products of syenites, to which they have transitional contacts (e.g.in Hurdal) (Pedersen 1986).

Both types occur in the central and north-

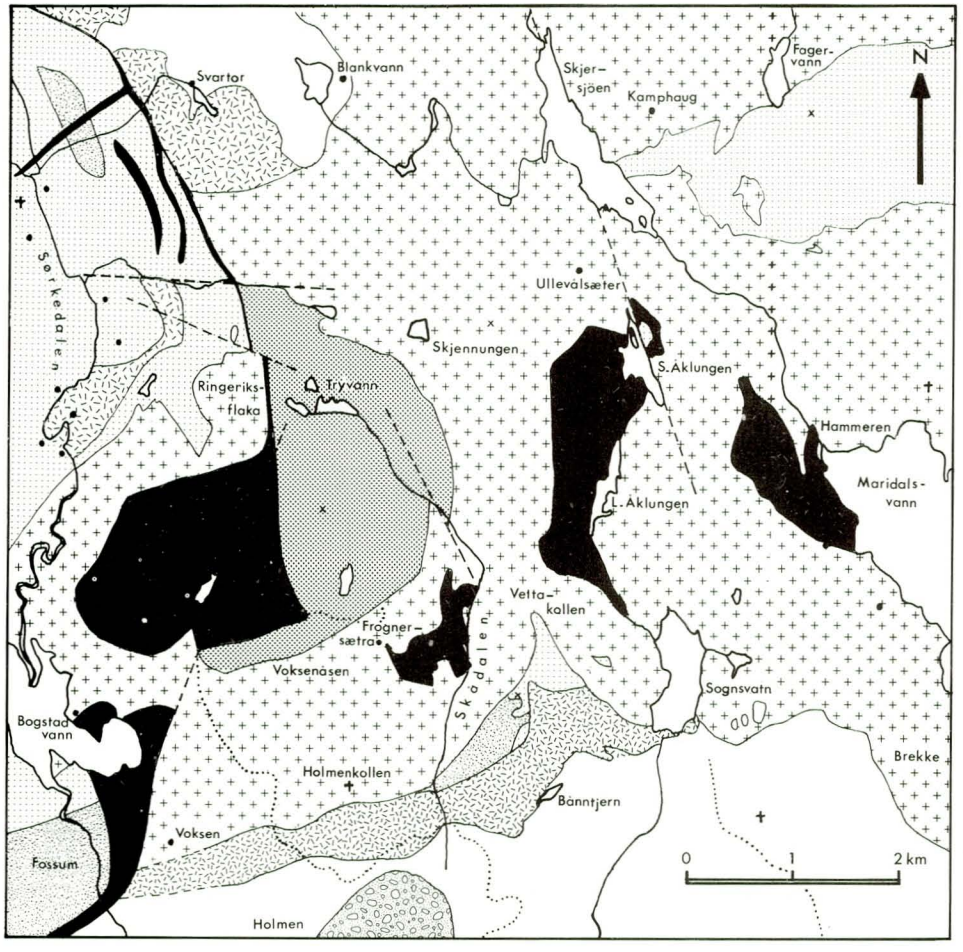


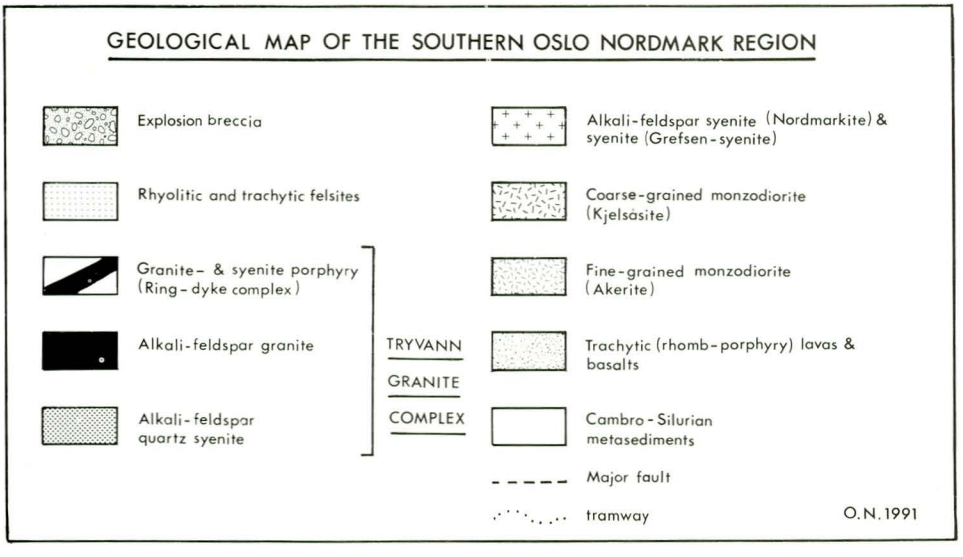


Fig. 2: Geological map of the southern Oslo Nordmark region.

ern part of the Oslo Graben and, together with alkali-feldspar syenites and alkali granites (ekerite), constitute most of the plutonic rocks in the Nordmarka-Hurdalen Syenite Complex of the Akershus Graben Segment (Ramberg 1976). In the Oslo district this plutonic complex borders the Cambro-Silurian metasediments of the lowland of Bærum and Oslo and the Bærum Cauldron (Fig.1). Geological maps of the area under consideration at 1:50 000 scale have been compiled by Holtedahl & Dons (1952) and Naterstad et al.(1990).

Between the lakes Bogstadvann and Maridalsvann four separate granite bodies intrude the different syenitic rocks of the Nordmarka-Hurdalen Syenite Complex (Fig.2). The Tryvann granite is the largest of these; and together with the intrusions at Skådalen, Åklungen and Hammeren it forms the *Tryvann Granite Complex (TGC)*, as revealed by the common field relations, petrology and geochemical composition of these four bodies.

The aim of this paper is to review the petrology and geochemistry of the TGC, with particular reference to the associated late- to post-magmatic hydrothermal ore mineralization. The tectonomagmatic relationship of the TGC with the Bærum Cauldron will be discussed. Some preliminary ideas on the association between the TGC and adjacent ore mineralizations associated with the late-magmatic episodes in the development of the Oslo Rift have previously been presented by Nilsen (1990).

## Geological setting

The Tryvann granite constitutes the major granitic body of the TGC, covering approximately 10km² of the hill Tryvannshøgda and the western hillside down to lake Bogstadvann (Fig.2). The petrography of this granite has previously been presented by Sæther (1962), Gaut (1981) and Petersen (1983), but no comprehensive geochemical accounts have yet been published. However, the Rb-Sr age determination of the granite at 241 ± 3 Ma by Sundvoll (1978), Sundvoll & Larsen (1990) and Sundvoll et al.(1990) has shown that the Tryvann granite represents one of the youngest magmatic rocks so far reported from the igneous complexes of the Oslo Rift.

The Tryvann granite constitutes a composite stock-shaped intrusion situated close to the eastern boundary of the Bærum Cauldron. It includes an eastern segment of medium- to fine-grained, partly porphyritic, alkali-feldspar quartz syenite, and a western segment of fine-grained, granophyric, alkali-feldspar granite of a greyish-pink colour. In the field the boundary between the two lithologies is transitional over a distance of approximately 100 m. The Skådalen, Åklungen and Hammeren Granites are satellite intrusions to the main Tryvann granite body. They are all fine-grained, granophyric, alkali-feldspar granites with irregular contacts.

The Tryvann granite has an important spatial and tectonomagmatic relationship with the Bærum Cauldron (Figs.1 & 3). The geology of the Bærum Cauldron has previously been described by Holtedahl (1943), Sæther (1945, 1962) and Oftedahl (1952,1953,1978). It has a semi-elliptic outline, measuring c. 8.5 x 10 km, and constitutes one of the best preserved cauldron structures of the Oslo Rift. It is composed of members of the younger lava series of the Oslo region which, in a pre-cauldron stage, were intersected by fine- and medium-grained monzodiorites (akerite), syenitic plutons and dykes, as well as hypabyssal porphyritic rhyolitic and syenitic felsites (e.g.the Lathus porphyry (Oftedahl 1946,1957), and the Sørkedal porphyry (Holtedahl 1943)). Subsequent igneous activity led to the formation of numerous igneous breccia vents, ignimbrites and volcaniclastic metasediments. To the west the cauldron borders the lava series at Kolsås and Krokskogen; to the north and to the east the various monzonitic and syenitic plutonic complexes of the Nordmarka-Hurdalen Syenite Complex; and to the south the Cambro-Silurian metasediments of the Oslo region.

The cauldron subsidence took place along a nearly vertical, cylindrical fault zone, less than 100m in width. Oftedahl (1953) has estimated a vertical subsidence of 600-700m in the southern part and approximately 1500m in the northern segment of the cauldron.

Along the cauldron boundary a prominent ring-dyke is exposed. The ring-dyke has a thickness of 20-100m and branches out as a concentric ring-dyke complex in the Sørkedalen area to the north of the cauldron where individual dykes may attain thicknesses of several hundred metres. The ring-dyke complex has steeply dipping boundaries against the

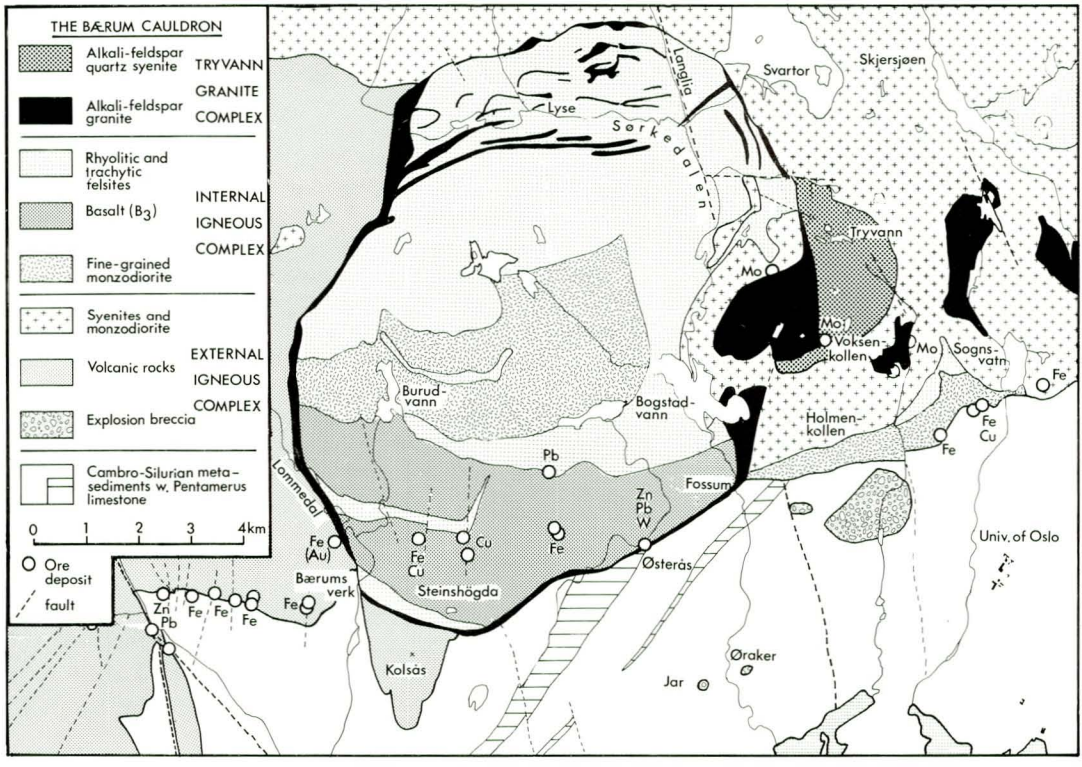


Fig. 3: Geological map of the Bærum Cauldron. Modified from Holtedahl & Dons (1952) and Naterstad et al.(1990).

adjacent wallrocks that are commonly brecciated. The dyke rocks appear undeformed and seem to have been emplaced after the subsidence of the cauldron block, and accordingly represent the last stage of igneous activity associated with the main subsidence of the Bærum Cauldron (Sæther 1945).

The ring dyke is basically developed as granophyric quartz porphyries, syenite porphyries and microgranites. An important feature of the Tryvann granite are its spatial and temporal relationships with the ring-dyke system of the Bærum Cauldron which can be studied in the Ringeriksflaka area to the west of lake Tryvann (Fig.2). Here the alkali-feldspar granite protrudes from the main Tryvann granite body and continues as a part of the ring-dyke, separating the alkali-feldspar quartz syenite in the east from the subsided raft of the older Grefsen syenite within the cauldron. The field relations reveal clearly that the emplacement of Tryvann granite took place after the subsidence of the Bærum Cauldron, but contemporaneously with the formation of the ring-dyke complex along the main cauldron fault zone. This is in accordance with earlier assumptions by Sæther (1945), Smithson (1961) and Petersen (1983) which have recently been supported by a Rb-Sr age of 243±3 Ma for the ring-dyke (Sundvoll et al.1990).

The contacts of the TGC with the enclosing syenites within and outside the cauldron are sharp and subvertical, often following the prominent fracture pattern of the area. The contacts to the surrounding plutonic rocks are in general characterized by sub-parallel apophyses and veins of porphyric aplites, 1-20 cm in thickness, protruding from the main granitic intrusions.

The plutonic rocks intruded by the TGC comprise a complex of alkali-feldspar syenites (nordmarkite), syenites (Grefsen syenite), fine- to medium-grained monzodiorites (akerite), and coarse-grained monzodiorites (kjelsåsite). The Grefsen syenite is an ordinary syenite, which is commonly developed as a plagioclase-phyric variety. It has been intruded by the Tryvann and Skådalen granites, while the

Åklungen and Hammeren bodies of the TGC intrude aphyric and commonly aegirine-bearing alkali-feldspar syenites (nordmarkite). Due to the indistinct field relationships between the two syenite types, no attempt has been made in this study to distinguish between them in the field. In the Oslo-Nittedal district, the field relationships suggest that the Grefsen syenites are older than the alkali-feldspar syenites, and this has been supported by the recent Rb-Sr datings, e.g. ± 255 Ma and ± 250 Ma for the Grefsen syenites and alkali-feldspar syenites, respectively (Sundvoll et al.1990).

Diabase dykes, 0.5-1.5m in thickness, transect the TGC and the Bærum Cauldron boundary in a few places. Their petrography has been presented by Sæther (1947) and Huseby (1971). They are regarded as the youngest magmatic rocks of the region and are controlled by the prominent N-S fracture system of the area.

To the south of the TGC and the Nordmarka-Hurdalen Syenite Complex the *Holmen-Dagali explosion-breccia* transects the Cambro-Silurian hornfels sequence in the area between Holmenkollen and Ullernåsen (Figs. 1,2 & 3). The breccia has briefly been presented by Holtedahl (1943,p.50) and Sæther (1962,p.94), and bears an interesting relationship to the TGC as it is composed of various angular and sub-rounded fragments of hydrothermally altered and unaltered varieties of fine-grained, granitic rocks, resembling the different lithologies of the TGC together with a variety of fragments of different lithologies from the Cambro-Silurian sequence, Precambrian gneisses and igneous rocks from the Nordmarka-Hurdalen Syenite complex. The rock-flour matrix consists of Cambro-Silurian shale and limestone close to the contact and of tuffaceous igneous material elsewhere. The formation of the breccia-pipe probably signifies the last magmatic event associated with the development of the TGC and will be considered later.

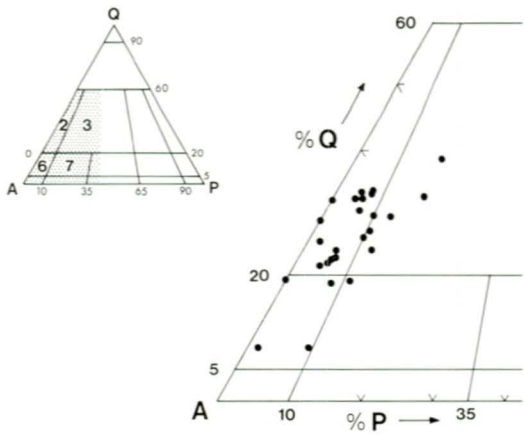


Fig. 4: Modal composition of the Tryvann Granite Complex, including data from Gaut (1981). Fields of classification: 2: Alkali-feldspar granite 3: Granite 6: Alkali-feldspar quartz syenite 7: Quartz syenite.

## Petrography of the Tryvann Granite Complex

### *Alkali-feldspar quartz syenite*

The alkali-feldspar quartz syenite which occupies the eastern part of the Tryvann granite is a greyish-pink, commonly porphyritic, fine-grained rock with a subhedral, granular texture. Perthitic K-feldspar, quartz and albite constitute more than 95 vol% of the rock. Brown biotite, partly chloritized, occurs in minor amounts (<3 vol%), along with accessory apatite, rutile, zircon, fluorite, sphene, magnetite, hematite, pyrite and ilmenite. Scattered xenocrysts of a greenish-grey amphibole with strongly abraded grain boundaries occur in some syenite varieties, presumably derived from the enclosing Grefsen syenite.

Phenocrysts of perthitic K-feldspar occur in general as scattered, randomly oriented, subhedral tablets, 2-7mm across and with a yellowish-grey colour in a fine-grained (0.2-1mm) granular matrix. The K-feldspar is developed as a braid- or patch-perthite, commonly showing a distinct Carlsbad-twinning. Albite occurs as subhedral separate grains in the matrix, but mainly occurs as cores within, or mantles around, the turbid zoned K-feldspar

grains and phenocrysts. Quartz forms anhedral interstitial grains, 0.2-0.6mm across and, less commonly, micrographic intergrowths with the K-feldspars. In the field the general porphyric texture and the low quartz content (15-20 vol.%) distinguish the alkali-feldspar quartz syenite from the alkali-feldspar granite, but transitional varieties are common in the border zone between them. Dark brown biotite occurs as scattered, randomly oriented, single flakes, 0.3-1mm in length, commonly associated with aggregates of fine-grained magnetite, apatite, rutile and sphene. The biotite is commonly replaced by a dark green chlorite along cleavage planes and grain boundaries. Sphene generally occurs as euhedral grains, commonly replacing magnetite and fine-grained aggregates of rutile. Zircon is a fairly common accessory mineral, and occurs as single, euhedral prisms, less than 0.3mm across.

## *Alkali-feldspar granite*

The alkali-feldspar granite differs petrographically from the alkali-feldspar quartz syenite by its general aphyric texture and higher quartz content (25-30 vol.%). Towards the western margin of the Tryvann granite miarolitic cavities, 2-10mm across, are commonly present, but no particular lateral or vertical compositional zoning is observed in the granite body.

The granite has a granophyric texture with an average grain size of between 0.1 and 1mm. The granophyric texture is defined by subhedral grains of quartz enclosing K-feldspar in a micrographic pattern. The mineralogical composition does not differ significantly from that of the alkali-feldspar quartz syenites. However, the Skådalen, Åklungen and Hammeren granites are significantly depleted in biotite and magnetite in comparison with the Tryvann granite. In places, arfvedsonite may occur as the predominant dark mineral constituent in amounts of less than 3 vol.% within the Skådalen and Hammeren granites, thereby indicating a gradation to peralkaline (ekeritic) varieties.

Albite replaces turbid K-feldspars in the alkali-feldspar granites to various degrees, and transitions to greyish-white albite granites are frequently observed. The role of hydrothermal alteration resulting in albitization of the TGC and surrounding rocks will be discussed in a later paragraph.

Modal analyses have been performed on 23 samples from the TGC (Table 1) and are presented in a Streckeisen diagram together with 6 analyses of the Tryvann granite from Gaut (1981)(Fig.4). Most samples cluster in the alkali-feldspar granite field of the diagram, but the more albitic varieties grade into the granite field. Due to the general porphyritic texture, only a limited number of alkali-feldspar quartz syenites were found suitable for modal analyses. However, these samples fall well within the alkali-feldspar quartz syenite field of the diagram.

Table 1: Modal composition of the Tryvann Granite Complex.

| ALKALI-FELDSPAR GRANITE | | | | | | | | | | | | | | | | | ALKALI-FELDSPAR QUARTZ SYENITE | | | | | | | |
|---|---|---|---|---|---|---|---|---|---|---|---|---|---|---|---|---|---|---|---|---|---|---|---|---|
| SAMPLE NO. | 2 | 3 | 4 | 7 | 28 | 33 | 36 | 50 | 64 | 93 | 107 | 109 | 113 | 134 | 138 | 141 | SAMPLE NO. | 39 | 40 | 41 | 47 | 53 | 55 | 58 |
| MINERAL (vol.%) | | | | | | | | | | | | | | | | | MINERAL (vol.%) | | | | | | | |
| Albite | 7.0 | 4.5 | 3.0 | 3.5 | 4.9 | 3.4 | 7.3 | 4.8 | 8.5 | 12.0 | 9.2 | 4.1 | 0.0 | 3.8 | 11.7 | 9.2 | Albite | 4.8 | 11.7 | 8.1 | 7.5 | 7.7 | 9.8 | 6.1 |
| Quartz | 29.0 | 30.0 | 31.5 | 33.0 | 33.1 | 20.4 | 24.7 | 32.4 | 18.4 | 30.7 | 23.3 | 21.3 | 27.9 | 30.8 | 37.4 | 28.4 | Quartz | 21.8 | 18.2 | 7.9 | 26.3 | 11.7 | 17.4 | 17.5 |
| Alkalifsp. | 62.0 | 64.5 | 63.0 | 63.0 | 61.1 | 70.8 | 64.2 | 61.0 | 70.0 | 51.5 | 65.1 | 72.3 | 69.3 | 61.2 | 48.4 | 59.5 | Alkalifsp. | 69.0 | 64.8 | 76.8 | 63.6 | 72.1 | 68.9 | 70.0 |
| Biotite/Chlorite | 1.0 | 0.5 | 0.5 | | 0.1 | 2.6 | 1.8 | 0.3 | 0.7 | | | 0.5 | 0.7 | | 0.1 | | Biotite/Chlorite | 2.5 | 1.7 | 2.1 | 0.6 | 1.5 | 1.3 | 2.2 |
| Arfvedsonite | | | | | | | | | 4.3 | | | | | 3.3 | | | Amphibole | | | 1.8 | | 3.4 | 0.6 | 1.1 |
| Apatite | x | | | | | | x | | x | | | | x | | | | Apatite | x | x | x | x | x | x | x |
| Rutile | x | | x | | | | x | | | | x | | x | | x | | Rutile | x | | | x | | | x |
| Zircon | x | | x | x | | x | x | x | x | | x | x | x | x | x | x | Zircon | x | x | x | x | x | x | x |
| Fluorspar | x | | | x | x | x | x | | | x | | x | | x | x | | Fluorspar | x | | | x | | | |
| Carbonate | | | | | | 1.1 | | | | x | | | | | | | Carbonate | | 1.5 | 0.8 | | 1.6 | 1.0 | 1.3 |
| Magnetite | | 0.5 | | 0.5 | 0.5 | 1.2 | 1.1 | 1.1 | 0.6 | 3.5 | 1.8 | 1.3 | 1.5 | 0.5 | 1.0 | 2.6 | Magnetite | 0.3 | 1.7 | 1.8 | 0.8 | 1.5 | 0.7 | 0.7 |
| Hematite | | | x | | | | | | | x | x | | | | 1.0 | x | Hematite | | | x | | | | |
| Pyrite | 1.0 | x | 2.0 | | | | x | | | | | | | | | | | | | | | | | |
| SUM | 100.0 | 100.0 | 100.0 | 100.0 | 99.7 | 99.5 | 99.1 | 99.6 | 102.5 | 97.7 | 99.4 | 99.5 | 99.4 | 99.6 | 99.6 | 99.7 | SUM | 98.4 | 99.6 | 99.3 | 98.8 | 99.5 | 99.7 | 98.9 |

x: Accessory constituent.

*Sample localities and bodies* — 2: Rødkleiva (top), Voksenkollen Tryvann. 3: Rødkleiva (middle), Voksenkollen - Tryvann. 4: Rødkleiva (bottom), Voksenkollen - Tryvann. 7: Wyllerløypa (top), Ringeriksflaka - Tryvann. 28: N. Strømsbråten, Sørkedalen - Tryvann. 33: Bus stop, Bogstad, Sørkedalen - Ring-dyke. 36: Hytlibakken, S. Tryvann - Tryvann. 50: Presterudhaugen, W. Tryvann - Tryvann. 64: Footpath Bomveien-Frognersætra - Skådal. 93: Heftyebakken, SE Tryvann - Skådal. 107: W. St. Åklungen - Åklungen. 109: W.L. Åklungen - Åklungen. 113: E. Måneskinnsløypa, Vettakollen - Åklungen. 134: Hammeren - Hammeren. 138: Skjervenmarka - Hammeren. 141: Skjerven Saw mill - Hammeren. 39: Tryvannskleiva, top. 40: Tryvann tower. 41: Grøttumskleivene. 47: Skogen station. 53: Pinslehøgda. 55: N. Heggehullet. 58: Tryvann.

## *The ring-dyke complex*

The petrography of the ring-dyke complex of the Bærum Cauldron has previously been presented by Sæther (1945) from the southern part of the cauldron. In general, the ring dyke is developed as a fine-grained, pinkish-grey quartz-syenite porphyry. Randomly oriented phenocrysts of subhedral alkali feldspar, 1-5 mm across, occur scattered in a very fine-grained, partly granophyric groundmass of quartz and alkali feldspar with albite in minor amounts. Rounded phenocrysts of quartz, less than 1mm across, may occur in places. Biotite, sphene, zircon, rutile, fluorite, apatite, hematite and pyrite are accessory constituents. In the southern part of the Bærum cauldron scattered xenoliths, 1-10 cm across, occur in the ring-dyke. They are composed of porphyritic basalts and various rhomb-porphyry lithologies from the central igneous complexes of the cauldron.

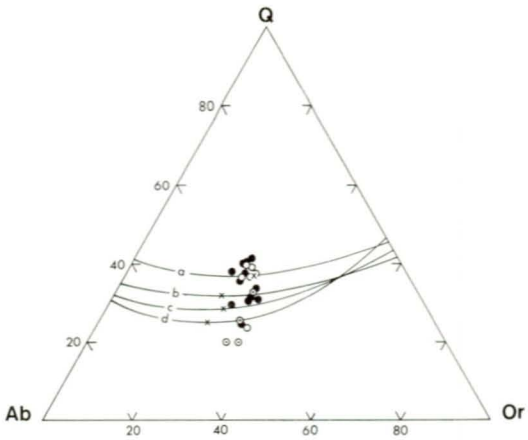


Fig. 6: Q-Or-Ab relations for the Tryvann Granite Complex. Cotectic lines with thermal minima (x) are shown for different volatile contents after Tuttle & Bowen (1958) and Manning (1981): a: 1 Kbar, 4.3% $H_2O$ b: 3 Kbar, 8% $H_2O$ c: 1 Kbar, 1% F d: 1 Kbar, 2% F. Symbols as in Figs.5 & 7.

## Analytical procedures and results

Thirty-two chemical analyses have been performed on the different lithologies of the TGC and the Bærum Cauldron ring-dyke complex (Tables 2 & 3). Major and minor elements were determined by X-ray fluorescence (XRF) analyses on a Philips instrument, using fused pellets made from rock powder mixed 1:9 with $LiB_4O_7$. The trace elements (Mo,Nb,Zr,Y, Sr,Rb,Ce and Ba) were analyzed on pressed

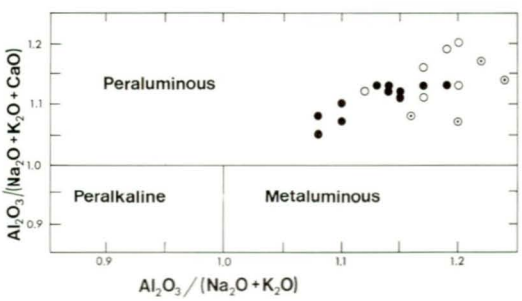


Fig. 5: $Al_2O_3/(Na_2O + K_2O)$ versus $Al_2O_3/(Na_2O + K_2O + CaO)$ of the Tryvann Granite Complex. Field boundaries according to Shand (Carmichael et al.1974). Oxide values are in molecular proportions. Legend: Circles with dot - Alkali-feldspar quartz syenite; Open circles - Ring-dyke; Filled circles - Alkali-feldspar granite.

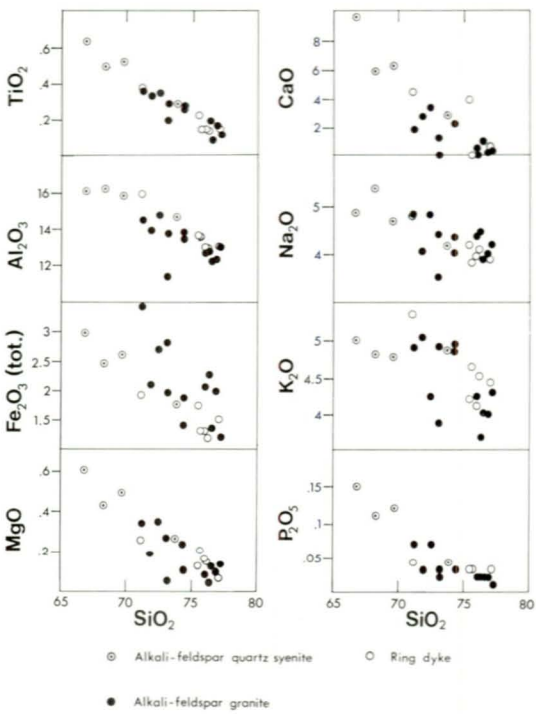


Fig. 7: Harker diagrams showing major and minor oxides from samples from the Tryvann Granite Complex and the Bærum Cauldron ring dyke complex. All figures are weight per cent values.

Table 2: Chemical analyses and CIPW norms of the Tryvann Granite Complex and the Bærum Cauldron ring dyke. All values are in wt.% except for trace elements, which are in ppm.

| ALKALI-FELDSPAR GRANITE | | | | | | | | | | | | | ALKALI-FELDSPAR QUARTZ SYENITE | | | | RING-DYKE | | | | |
|---|---|---|---|---|---|---|---|---|---|---|---|---|---|---|---|---|---|---|---|---|---|
| SAMPLE NO. | 2 | 4 | 28 | 36 | 64 | 93 | 107 | 109 | 113 | 134 | 138 | 141 | 40 | 47 | 53 | 58 | 50 | 7 | L07 | L11 | L37 | L38 |
| $SiO_2$ | 74.35 | 77.18 | 76.50 | 72.50 | 71.25 | 73.10 | 73.16 | 71.88 | 74.36 | 76.02 | 76.85 | 76.32 | 68.34 | 73.84 | 66.87 | 69.72 | 77.08 | 75.46 | 71.17 | 76.02 | 76.20 | 75.68 |
| $TiO_2$ | 0.26 | 0.12 | 0.09 | 0.35 | 0.36 | 0.20 | 0.29 | 0.33 | 0.28 | 0.14 | 0.17 | 0.20 | 0.49 | 0.29 | 0.63 | 0.52 | 0.15 | 0.23 | 0.38 | 0.15 | 0.14 | 0.15 |
| $Al_2O_3$ | 13.81 | 13.02 | 12.21 | 14.77 | 14.51 | 11.39 | 13.76 | 13.91 | 13.46 | 12.68 | 12.35 | 12.78 | 16.20 | 14.67 | 16.07 | 15.83 | 13.04 | 13.64 | 15.95 | 13.01 | 12.98 | 13.56 |
| $Fe_2O_3$* | 1.41 | 1.20 | 1.35 | 2.69 | 3.44 | 2.81 | 1.96 | 2.10 | 1.88 | 2.06 | 1.98 | 2.27 | 2.46 | 1.76 | 2.98 | 2.61 | 1.50 | 1.74 | 1.92 | 1.30 | 1.18 | 1.30 |
| MnO | 0.05 | 0.05 | 0.05 | 0.12 | 0.21 | 0.27 | 0.14 | 0.12 | 0.12 | 0.13 | 0.17 | 0.17 | 0.10 | 0.05 | 0.11 | 0.08 | 0.05 | 0.11 | 0.12 | 0.03 | 0.02 | 0.04 |
| MgO | 0.24 | 0.13 | 0.12 | 0.35 | 0.34 | 0.27 | 0.05 | 0.19 | 0.10 | 0.08 | 0.09 | 0.04 | 0.43 | 0.27 | 0.60 | 0.49 | 0.06 | 0.12 | 0.26 | 0.16 | 0.14 | 0.21 |
| CaO | 0.22 | 0.03 | 0.10 | 0.33 | 0.18 | 0.12 | 0.00 | 0.27 | 0.22 | 0.05 | 0.02 | 0.00 | 0.58 | 0.28 | 0.95 | 0.62 | 0.06 | 0.39 | 0.44 | 0.00 | 0.00 | 0.00 |
| $Na_2O$ | 4.00 | 4.17 | 3.86 | 4.79 | 4.81 | 3.50 | 4.37 | 4.02 | 4.32 | 4.33 | 3.98 | 4.44 | 5.33 | 4.14 | 4.83 | 4.65 | 3.86 | 4.15 | 4.75 | 3.92 | 4.06 | 3.79 |
| $K_2O$ | 4.83 | 4.28 | 4.00 | 4.22 | 4.89 | 3.86 | 4.90 | 5.03 | 4.93 | 4.22 | 3.98 | 3.66 | 4.80 | 4.85 | 4.98 | 4.76 | 4.41 | 4.18 | 5.33 | 4.09 | 4.50 | 4.63 |
| $P_2O_5$ | 0.03 | 0.01 | 0.02 | 0.07 | 0.07 | 0.03 | 0.02 | 0.03 | 0.03 | 0.02 | 0.02 | 0.02 | 0.11 | 0.04 | 0.15 | 0.12 | 0.03 | 0.03 | 0.04 | 0.02 | 0.02 | 0.03 |
| S | 0.11 | 0.01 | 0.01 | 0.26 | 0.01 | 0.08 | 0.01 | 0.01 | 0.01 | 0.01 | 0.01 | 0.01 | 0.01 | 0.01 | 0.01 | 0.01 | 0.01 | 0.00 | 0.00 | 0.04 | 0.01 | 0.01 |
| LOI | 0.41 | 0.16 | 0.23 | 0.67 | 0.27 | 2.91 | 0.24 | 0.56 | 0.49 | 0.45 | 0.26 | 0.18 | 0.39 | 0.42 | 0.25 | 0.38 | 0.24 | 1.08 | 0.52 | 0.19 | 0.20 | 0.26 |
| **SUM** | **99.72** | **100.36** | **98.54** | **101.12** | **100.34** | **98.54** | **98.90** | **98.45** | **100.20** | **100.19** | **99.88** | **100.09** | **99.24** | **100.62** | **98.43** | **99.79** | **100.49** | **101.13** | **100.88** | **98.93** | **99.45** | **99.66** |
| Mo | 11 | 13 | 9 | 19 | 21 | 0 | 2 | 5 | 6 | 43 | 8 | 0 | 9 | 12 | 4 | 7 | 22 | 15 | 1 | 9 | 10 | 8 |
| Nb | 84 | 94 | 141 | 89 | 174 | 218 | 194 | 160 | 158 | 241 | 162 | 217 | 88 | 90 | 95 | 78 | 85 | 157 | 92 | 101 | 101 | 95 |
| Zr | 244 | 169 | 209 | 312 | 560 | 714 | 621 | 414 | 383 | 469 | 402 | 619 | 391 | 274 | 458 | 371 | 169 | 400 | 634 | 204 | 201 | 199 |
| Y | 45 | 31 | 29 | 36 | 102 | 131 | 55 | 96 | 82 | 109 | 55 | 82 | 58 | 50 | 66 | 57 | 22 | 56 | 81 | 36 | 35 | 35 |
| Sr | 31 | 8 | 5 | 74 | 42 | 14 | 19 | 20 | 31 | 5 | 4 | 5 | 144 | 47 | 150 | 165 | 12 | 27 | 31 | 60 | 24 | 67 |
| Rb | 243 | 228 | 259 | 188 | 211 | 239 | 204 | 233 | 225 | 294 | 230 | 191 | 180 | 227 | 144 | 163 | 220 | 186 | 140 | 145 | 211 | 203 |
| Ce | 183 | 81 | 74 | 143 | 368 | 150 | 174 | 219 | 209 | 113 | 116 | 138 | 151 | 156 | 145 | 151 | 82 | 129 | 220 | 93 | 81 | 85 |
| Ba | 157 | 79 | 0 | 411 | 474 | 132 | 123 | 92 | 175 | 20 | 10 | 25 | 667 | 275 | 720 | 726 | 58 | 148 | 158 | 83 | 45 | 58 |

| CIPW-NORM | | | | | | | | | | | | | CIPW-NORM | | | | | | | | | |
|---|---|---|---|---|---|---|---|---|---|---|---|---|---|---|---|---|---|---|---|---|---|---|
| SAMPLE NO. | 2 | 4 | 28 | 36 | 64 | 93 | 107 | 109 | 113 | 134 | 138 | 141 | 40 | 47 | 53 | 58 | 50 | 7 | L07 | L11 | L37 | L38 |
| Q | 32.12 | 36.29 | 39.10 | 27.39 | 23.37 | 39.09 | 29.36 | 29.13 | 29.97 | 34.61 | 38.48 | 36.48 | 17.65 | 30.65 | 17.58 | 22.92 | 37.57 | 34.43 | 21.89 | 37.85 | 35.46 | 35.86 |
| Or | 28.78 | 25.28 | 24.08 | 24.87 | 28.98 | 23.90 | 29.40 | 30.42 | 29.27 | 25.04 | 23.65 | 21.69 | 28.75 | 28.65 | 30.04 | 28.39 | 26.03 | 24.73 | 31.44 | 24.51 | 26.83 | 27.57 |
| Al | 34.06 | 35.19 | 33.20 | 40.34 | 40.67 | 30.96 | 37.46 | 34.74 | 36.64 | 36.72 | 33.79 | 37.59 | 45.61 | 34.94 | 41.62 | 39.57 | 32.56 | 35.08 | 40.03 | 33.57 | 34.59 | 32.24 |
| An | 0.90 | 0.08 | 0.37 | 1.18 | 0.44 | 0.42 | 0.00 | 1.17 | 0.90 | 0.12 | 0.00 | 0.00 | 2.19 | 1.13 | 3.81 | 2.31 | 0.01 | 1.74 | 1.92 | 0.00 | 0.00 | 0.00 |
| C | 1.67 | 1.48 | 1.41 | 1.87 | 1.13 | 1.36 | 1.27 | 1.45 | 0.68 | 0.94 | 1.49 | 1.51 | 1.45 | 0.18 | 1.38 | 2.19 | 1.86 | 1.64 | 1.64 | 2.15 | 1.43 | 2.32 |
| Di | 0.00 | 0.00 | 0.00 | 0.00 | 0.00 | 0.00 | 0.00 | 0.00 | 0.00 | 0.00 | 0.00 | 0.00 | 0.00 | 0.00 | 0.00 | 0.00 | 0.00 | 0.00 | 0.65 | 0.41 | 0.00 | 0.53 |
| Wo | 0.00 | 0.00 | 0.00 | 0.00 | 0.00 | 0.00 | 0.00 | 0.00 | 0.00 | 0.00 | 0.00 | 0.00 | 0.00 | 0.00 | 0.00 | 0.00 | 0.00 | 0.00 | 0.00 | 0.00 | 0.00 | 0.00 |
| Hy | 0.60 | 0.32 | 0.33 | 0.87 | 0.85 | 0.89 | 0.13 | 0.49 | 0.25 | 0.31 | 0.36 | 2.00 | 1.09 | 0.67 | 1.53 | 1.23 | 0.15 | 0.30 | 0.00 | 0.00 | 0.35 | 0.00 |
| Mt | 0.52 | 1.01 | 1.28 | 1.22 | 3.17 | 2.59 | 1.63 | 1.61 | 1.50 | 1.93 | 1.85 | 2.18 | 1.44 | 1.11 | 1.61 | 1.43 | 1.25 | 1.49 | 1.27 | 0.88 | 0.85 | 1.01 |
| Hm | 0.55 | 0.70 | 0.00 | 0.89 | 0.03 | 0.00 | 0.15 | 0.27 | 0.18 | 0.00 | 0.00 | 0.00 | 0.61 | 0.37 | 0.84 | 0.70 | 0.10 | 0.09 | 0.35 | 0.24 | 0.18 | 0.14 |
| Il | 0.50 | 0.23 | 0.15 | 0.66 | 0.68 | 0.40 | 0.56 | 0.64 | 0.53 | 0.27 | 0.32 | 0.38 | 0.94 | 0.55 | 1.22 | 0.99 | 0.28 | 0.44 | 0.72 | 0.29 | 0.27 | 0.29 |
| Py | 0.21 | 0.02 | 0.02 | 0.49 | 0.02 | 0.16 | 0.02 | 0.02 | 0.02 | 0.02 | 0.02 | 0.02 | 0.02 | 0.02 | 0.02 | 0.02 | 0.02 | 0.00 | 0.00 | 0.08 | 0.02 | 0.02 |
| Ap | 0.07 | 0.02 | 0.05 | 0.17 | 0.17 | 0.07 | 0.00 | 0.07 | 0.07 | 0.05 | 0.05 | 0.00 | 0.26 | 0.09 | 0.36 | 0.29 | 0.07 | 0.07 | 0.09 | 0.00 | 0.00 | 0.00 |
| **SUM** | **99.98** | **100.62** | **99.99** | **99.95** | **99.51** | **99.84** | **99.98** | **100.01** | **100.01** | **100.01** | **100.01** | **101.85** | **100.01** | **98.36** | **100.01** | **100.04** | **99.90** | **100.01** | **100.00** | **99.98** | **99.98** | **99.98** |

* Total Fe as $Fe_2O_3$

Sample localities and bodies - 2: Rødkleiva (top), Voksenkollen, Tryvann. 4: Rødkleiva (bottom), Voksenkollen, Tryvann. 28: N. Strømsbråten, Sørkedalen, Tryvann. **36**: N. Hytlibakken, S. Tryvann, Tryvann. 64: Footpath Bomveien-Frognersætra, Skådal. 93: Heftyebakken, SE Tryvann, Skådal. 107: W. St. Åklungen, Åklungen. **109: W.L.** Åklungen, Åklungen. 113: E. Måneskinnsløypa, Vettakollen, Åklungen. 134: Hammeren, Hammeren. 138: Skjervenmarka, Hammeren. 141: Skjerven sag, Hammeren. **40:** Tryvann tower. **47:** Skogen station. 53: Pinslehøgda. 58: Tryvann. 50: Presterudhaugen, W. Tryvann. 7: Østerås (87J4/10). L07: NW Pipenhus, Sørkedalen. L11: **NW Pipenhus, Sørkedalen.** L37: Road S. Lysedammene, Sørkedalen. L38: Gran, Sørkedalen.

Table 3: Chemical analyses of hydrothermally altered varieties (A) of the Tryvann Granite Complex, enclosing syenites and the Bærum Cauldron ring dyke with their adjacent, unaltered protores (U). All values are in wt.%, except for trace elements, which are in ppm.

| ALKALI-FELDSPAR GRANITE | | | | | | | | | | | RING-DYKE | | GREFSEN-SYENITE | | | |
|---|---|---|---|---|---|---|---|---|---|---|---|---|---|---|---|---|
| SAMPLE NO. | U 64 | A 65 | U 109 | A 108 | U 141 | A 142 | U 2 | A A2 | U 4 | A A4 | U 7 | A 1 | U 48 | A 49 | U 132 | A 133 |
| $SiO_2$ | 71.25 | 55.27 | 71.88 | 75.49 | 76.32 | 75.34 | 74.35 | 69.75 | 77.18 | 78.44 | 75.46 | 73.56 | 66.70 | 62.79 | 64.09 | 71.91 |
| $TiO_2$ | 0.36 | 0.38 | 0.33 | 0.28 | 0.20 | 0.21 | 0.26 | 0.30 | 0.12 | 0.11 | 0.23 | 0.24 | 0.48 | 0.63 | 0.73 | 0.59 |
| $Al_2O_3$ | 14.51 | 13.95 | 13.91 | 13.31 | 12.78 | 12.59 | 13.81 | 14.98 | 13.02 | 12.71 | 13.64 | 13.31 | 16.84 | 16.59 | 16.92 | 16.49 |
| $Fe_2O_3$* | 3.44 | 3.94 | 2.10 | 2.00 | 2.27 | 2.20 | 1.41 | 3.53 | 1.20 | 1.04 | 1.74 | 1.87 | 2.86 | 3.32 | 3.14 | 0.77 |
| MnO | 0.21 | 3.44 | 0.12 | 0.15 | 0.17 | 0.08 | 0.05 | 0.02 | 0.05 | 0.38 | 0.11 | 0.10 | 0.14 | 0.69 | 0.17 | 0.03 |
| MgO | 0.34 | 0.04 | 0.19 | 0.21 | 0.04 | 0.11 | 0.24 | 0.13 | 0.13 | 0.13 | 0.12 | 0.14 | 0.50 | 0.60 | 0.66 | 0.16 |
| CaO | 0.18 | 0.70 | 0.27 | 0.04 | 0.00 | 0.00 | 0.22 | 0.00 | 0.03 | 0.00 | 0.39 | 0.39 | 0.80 | 1.62 | 0.59 | 0.02 |
| $Na_2O$ | 4.81 | 7.94 | 4.02 | 7.49 | 4.44 | 6.96 | 4.00 | 8.32 | 4.17 | 6.60 | 4.15 | 4.16 | 5.59 | 9.24 | 5.88 | 9.14 |
| $K_2O$ | 4.89 | 0.28 | 5.03 | 0.07 | 3.66 | 0.02 | 4.83 | 0.16 | 4.28 | 0.05 | 4.18 | 4.26 | 5.44 | 0.13 | 5.07 | 0.06 |
| $P_2O_5$ | 0.07 | 0.10 | 0.03 | 0.03 | 0.02 | 0.02 | 0.03 | 0.03 | 0.01 | 0.01 | 0.03 | 0.04 | 0.09 | 0.15 | 0.16 | 0.03 |
| S | 0.01 | 1.31 | 0.01 | 0.01 | 0.01 | 0.01 | 0.11 | 0.98 | 0.01 | 0.00 | 0.00 | 0.44 | 0.18 | 0.08 | 0.02 | 0.01 |
| LOI | 0.27 | 2.45 | 0.56 | 0.22 | 0.18 | 0.26 | 0.41 | 1.54 | 0.16 | 0.36 | 1.08 | 0.90 | 0.34 | 2.08 | 0.36 | 0.45 |
| **SUM** | **100.34** | **89.80** | **98.45** | **99.30** | **100.09** | **97.80** | **99.72** | **99.74** | **100.36** | **99.83** | **101.13** | **99.41** | **99.96** | **97.92** | **97.79** | **99.66** |
| Mo | 21 | 4 | 5 | 3 | 0 | 3 | 11 | 113 | 13 | 10 | 15 | 14 | 2 | 1 | 2 | 6 |
| Nb | 174 | 119 | 160 | 169 | 217 | 203 | 84 | 105 | 94 | 103 | 157 | 153 | 100 | 76 | 95 | 177 |
| Zr | 560 | 438 | 414 | 437 | 619 | 554 | 244 | 283 | 169 | 156 | 400 | 392 | 691 | 575 | 500 | 857 |
| Y | 102 | 40 | 96 | 93 | 82 | 66 | 45 | 32 | 31 | 20 | 56 | 57 | 97 | 66 | 74 | 49 |
| Sr | 42 | 1093 | 20 | 13 | 5 | 8 | 31 | 13 | 8 | 11 | 27 | 40 | 62 | 149 | 201 | 11 |
| Rb | 211 | 16 | 233 | 4 | 191 | 3 | 243 | 5 | 228 | 2 | 186 | 207 | 122 | 5 | 113 | 4 |
| Ce | 368 | 280 | 219 | 179 | 138 | 99 | 183 | 91 | 81 | 68 | 129 | 127 | 372 | 230 | 245 | 107 |
| Ba | 474 | 39000 | 92 | 43 | 25 | 19 | 157 | 19 | 79 | 10 | 148 | 215 | 396 | 161 | 2380 | 57 |

* Total Fe as $Fe_2O_3$

Sample pairs and localities – 64/65: Frognersætra. 109/108: W.L. Åklungen. 141/142: Skjerven saw mill, Hammeren. 2/A2: Rødkleiva (top), Voksenkollen. 4/A4: Rødkleiva (bottom), Voksenkollen. 7/1: Østerås. 48/49: Skogen. 132/133: S.S. Åklungen.

powder pellets. All analytical data were obtained at the Department of Geology, Oslo.

The unaltered TGC alkali-feldspar granites, alkali-feldspar quartz syenites and the ring-dyke lithologies (Table 2) demonstrate the distinct peraluminous character of the complex, in accordance with Carmichael et al.(1974)(Fig 5). When plotted into the ternary Q-Ab-Or system (Fig.6), the majority of the lithologies fall in the low-pressure thermal valley, close to the thermal minimum on the cotectic line for 1 Kbar and 4% $H_2O$ (Tuttle & Bowen 1958), thus suggesting a residual melt origin for the granites and ring-dyke.

The co-variation of different element oxides with $SiO_2$ of the different members of the Tryvann Granite Complex are presented in Fig.7. It shows that decreasing trends exist for all major and minor elements, except for $K_2O$, $Na_2O$, $Fe_2O_3$(tot.) and CaO where a considerable scatter occurs. This may partly be due to incipient, secondary, hydrothermal alteration processes (e.g. albitization) which have affected the complex to different degrees. Titanium, in contrast, is relatively stable against alteration, and will be concentrated in the early fractions during crystallization of a granitoid magma. The smooth co-variation of $TiO_2$ vs. $K_2O$/Rb of the TGC lithologies (Fig.8) supports the contention that all members of the complex are part of a cogenetic suite, where a general differentiation trend from the alkali-feldspar quartz syenites into alkali-feldspar granite and ring-dyke rocks seems to exist. From the petrographic and geochemical considerations, the TGC rocks apparently represent end-products of a strongly differentiated granitic magma. This is also revealed in the Rb-Ba-Sr relationship of the rocks, which are strongly enriched in Rb with respect to Ba and Sr (Fig.9). The concentrations of the trace elements Y,Ce,Zr and Nb of the unaltered members of the TGC vary considerably, but no systematic variation with the $SiO_2$ contents can be found (Fig.10). However, the alkali-feldspar granite is in general characterized by higher concentrations of the actual elements.

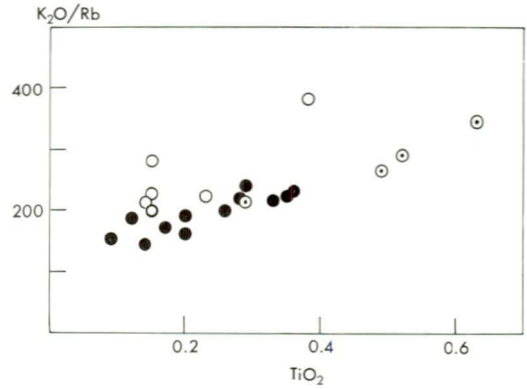


Fig. 8: $K_2O$/Rb ratios plotted against $TiO_2$ content (wt.%) from the Tryvann Granite Complex. Symbols as in Figs.5 & 7.

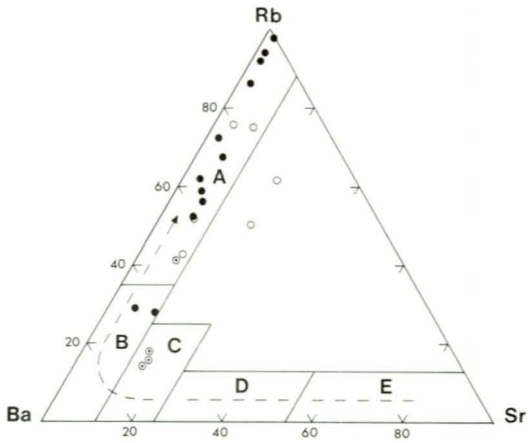


Fig. 9: Rb-Ba-Sr relations for the Tryvann Granite Complex. Fields of different rock types from the ternary model diagram of El Bouseily & El Sokkary (1975). Field A: Strongly differentiated granites; B: Normal granites; C: Anomalous granites; D: Granodiorites and quartz diorites; E: Diorites. Symbols as in Figs.5 & 7.

## Hydrothermal alteration

The alkali-feldspar granites of the TGC, the adjacent Grefsen syenite and the ring-dyke complex have locally been subjected to a conspicuous late- to post-magmatic hydrothermal alteration, commonly in close association with ore mineralizations. The hydrothermal alteration is mainly confined to prominent fracture zones, minor faults and, in places, at the contact to the adjacent older syenites. Within the alkali-feldspar granite, hydrothermal alteration has occurred along a great number of dis-

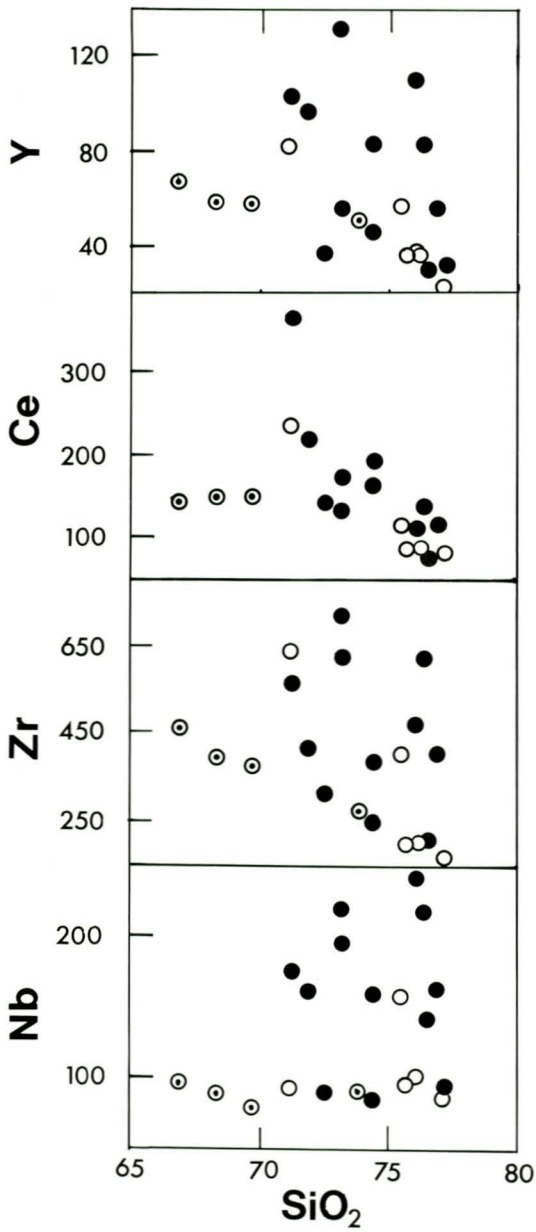


Fig. 10: Y,Ce,Zr and Nb (in ppm) versus $SiO_2$ (wt.%) of the Tryvann Granite Complex. Symbols as in Figs.5 & 7.

Fig. 11: Albitized zones in alkali-feldspar granite, Rødkleiva, Voksenåsen.

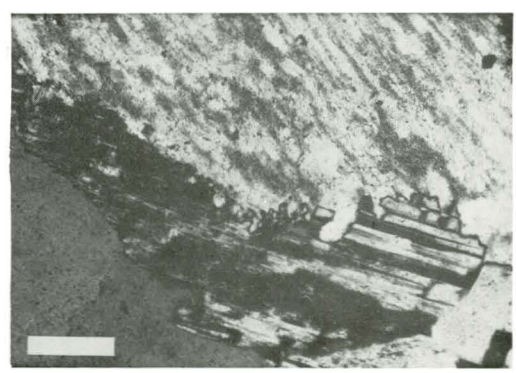

Fig. 12: Albitization of K-feldspar (turbid). Alkali-feldspar granite, W.St.Åklungen (specimen no.106). Crossed nicols. Scale bar: 0.1mm.

tinct, subparallel and steeply inclined fractures. They show bleached alteration envelopes with a thickness of 1 cm to several decimetres. Such fracture-controlled alteration is most prominently developed within the Tryvann granite, but also occurs in the Skådalen, Åklungen and Hammeren granites.

The fractures occur at all scales, from hairline healed cracks to veins with selvages of alteration many centimetres in width. The fractures have smooth walls which are parallel over many metres of dip and strike with a general uniform width of the alteration selvages (Fig. 11). The smooth parallel walls of the veins

indicate no transport or rotation of the blocks contained in the sheeted fracture system. In most of the alteration veins a prominent albitization has taken place as a volume-for-volume replacement of K-feldspar by albite (Fig.12). Albite usually shows a development of chess-board twinning. Within the granite, the albitization process is generally characterized by a textural change from granophyric, equigranular, perthitic alkali-feldspar granite to a fine-grained, saccharoidal albite granite. The dark minerals are commonly replaced by sulphides and iron-oxides. Similar fracture-bound albitic alteration has also been observed within the adjacent Grefsen syenite, close to the TGC-contact (e.g. Skogen station), but the frequency of veins decreases rapidly away from the contact. Small domains of a greyish-white albite granite, with outcrops covering 200-2000 m², occur locally within the Tryvann, Skådalen and Åklungen granites. They have transitional boundaries to the adjacent, pinkish alkali-feldspar granite, but do not show any apparent spatial relationship with the fracture-controlled albitic alteration. However, these albite granites show the same petrographical and textural relationships as the fracture-bound albitic alteration. In the albitized domains of the Skådalen granite, scapolite may locally replace the newly formed albite.

At the Bærum Cauldron boundary fault, between lake Bogstadvann and Tryvann, a major displacement of the Grefsen syenite has taken place as shown by the presence of a prominent fault-breccia, several metres in thickness (Fig.2). The fault-breccia has suffered a pervasive albitic alteration, as revealed by the presence of chess-board albite, formed at the expense of the original perthite in the clasts as well as in the matrix of the syenite-breccia.

A number of samples from the albitic veins and domains within the TGC and the bordering syenites have been selected, together with the immediately adjacent and unaltered lithologies, for chemical analysis. The geochemical data (Table 3) indicate that the alteration processes are characterized by a major change in alkali element ratios. The albitization of the different lithologies is revealed by an abrupt increase of normative albite at the expense of normative K-feldspar, while the normative quartz-content remains virtually unchanged or may even show a slight decrease during the albitization (Fig.13). Similar trends

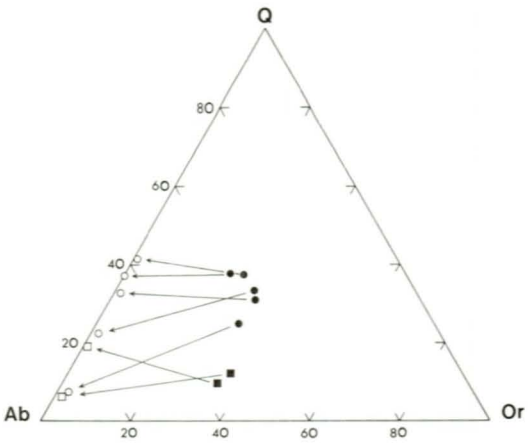


Fig. 13: Q-Or-Ab relations for unaltered and adjacent albitized alkali-feldspar granites of the Tryvann Granite Complex and Grefsen syenite. Squares - Grefsen syenite; circles - Alkali-feldspar granite. Filled symbols - Unaltered rocks; open symbols - Albitized rocks.

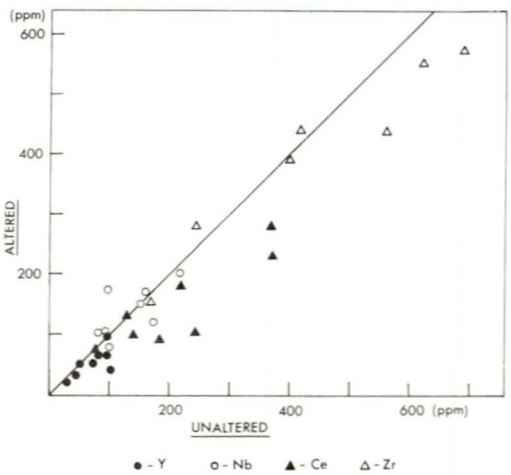


Fig. 14: Relationships between Y,Nb,Ce and Zr in altered and adjacent unaltered specimens from the Tryvann Granite Complex.

of albitization have been described by Kinnaird (1985) and Kinnaird et al.(1985) from the Mesozoic A-type granites of Nigeria. The trace elements Nb, Zr, and especially Y and Ce are slightly depleted during the albitization, as shown in Fig.14.

A trapped, Na-dominated, alkaline fluid phase may locally have caused a partial autometasomatism of the alkali-feldspar granites, giving rise to the domains of albite granite within the

Tryvann and Åklungen granites. Depending on the circumstance of crystallization, fluid escape or retention, the different styles of albitization may develop, as discussed by Bowden (1982) from the albitized Nigerian granites.

The effects of albitization appear to be most widespread within the central parts of the different granites of the TGC. Other types of hydrothermal alteration occur locally in association with vein-ore mineralizations at the exocontact zones of the Tryvann granite and the ring-dyke complex. Hence, potassic alteration is restricted to molybdenite-quartz veins crossing the Grefsen syenite — Tryvann granite boundary in the Ringeriksflaka area (Fig.2). Here, fine-grained K-feldspar forms alteration selvages, 1 to 2mm wide, marginal to the molybdenite veins which cross-cut zones of a brecciated, fine-grained, pyrite-topaz-fluorite-albite-quartz rock within the Grefsen syenite.

In the southern part of the Bærum cauldron extensive hydrothermal alteration with associated sulphide and oxide mineralizations have taken place inside the ring-dyke and close to the contact to the brecciated Cambro-Silurian metasediments. The hydrothermal alteration of the quartz syenite porphyry ring-dyke in the Fossum - Østerås area is revealed in an albitization (bleaching) of K-feldspar and by the replacement of disseminated, fine-grained hematite dust within the feldspars by magnetite. The pinkish ring-dyke attains a grey colour against the brecciated contact to the hornfelsed Cambro-Silurian metasediments which locally, is developed as a diopside-andradite skarn. At the contact, a replacement of the abundant K-feldspar phenocrysts of the dyke by epidote and/or sericite has occurred, and is succeeded by late deposition of carbonate, chlorite and sulphides (sphalerite, pyrite and minor galena), usually along irregular fissures and veins towards the contact.

Similar hydrothermal alteration processes (e.g. propylitization) have also locally affected the internal and external lava flows of the southern part of the cauldron boundary and are, in all probability, related to the late- or post-magmatic events of the Bærum Cauldron. The alteration zones are here chiefly confined to the several vein-type sulphide- and oxide-ore deposits in the Bærum district (Fig.3).

## Ore mineralization

Ore mineralizations are commonly developed in association with the alteration zones within the TGC, the adjacent Grefsen syenite and along the ring-dyke/Cambro-Silurian boundary. They can be separated into the following types:

1. Vertical veins and fissure coatings, 0.5-5mm thick, composed of fine-grained magnetite, hematite, ilmenite ± pyrite ± molybdenite with albitized wall-rock envelopes.

2. Composite pyrite ± molybdenite-bearing quartz veins, 1-10 mm thick, with fine-grained magnetite ± hematite ± ilmenite selvages against an albitic envelope.

3. Flaky molybdenite, occurring as 1-5 mm thick veins in the Grefsen syenite, close to the Tryvann granite boundary, which commonly cross-cut zones of microbrecciated topaz-albite-quartz rock with pyrite dissemination.

4. Disseminations of pyrite ± hematite ± flaky molybdenite in either unaltered or albititic (partly scapolitized) granite.

5. Veins and disseminations of sphalerite, pyrite, galena, hematite, chalcopyrite and scheelite, occurring as endo- and exoskarn mineralizations associated with albitized and propylitized ring-dyke.

The vein-type oxide/sulphide mineralizations (type 1) of the Tryvann granite are chiefly restricted to the central part of the granite, close to the bordering alkali-feldspar quartz syenite. The oxide ores comprise magnetite and hematite, with a grain size of 0.2-0.5 mm, with minor ilmenite and rutile. Hematite replaces magnetite as lamellar intergrowths and as aggregates coating the magnetite grains. Martitization of the magnetite and alteration of ilmenite into rutile ± hematite are common within the sulphide-free veins in the Åklungen and Hammeren granite bodies. Irregular joints coated with hematite ± magnetite accompany the strongly brecciated and albitized Grefsen syenite at the eastern Bærum Cauldron boundary at Bogstadlia to the east of lake Bogstadvann.

The sulphides (pyrite ± molybdenite) commonly replace the oxide ore assemblages in

the type (1)-veins in the Tryvann granite. Here, pyrite occurs as fine-grained disseminations with a grain size of 0.1 - 1 mm in the central part of the albitic veins. In the Voksenåsen area molybdenite often forms a microgranular 'moly-paint' upon the jointed surfaces of the fissured albite granite. The alkali-feldspar quartz syenite and the Åklungen and Hammeren granites are virtually free of any sulphide mineralizations; instead, hematite and/or magnetite veins and disseminations commonly accompany the albitic alteration zones.

The effect of the later sulphide mineralizing event succeeding the hydrothermal alteration and oxide mineralizations can be seen in the type (2) mineralized veins. These veins are chiefly restricted to the western (and deeper) part of the Tryvann granite where miarolitic cavities are abundant. Here, the oxide mineral assemblages (magnetite ± hematite) form thin (< 1 mm), symmetrical selvages upon the sulphide-bearing comb-textured and crustified quartz veins, indicating the opening of an oxide-mineralized fissure (type (1)) followed by an infilling of quartz and sulphides. Within the quartz veins, pyrite occurs as small subhedral to euhedral cubes with a grain size of 0.1 - 1mm. Within the pyrite, blebs of chalcopyrite and pyrrhotite may occur as well as tiny molybdenite flakes.

On blasted outcrops at the slalom hill Wyllerløypa at Ringeriks-flaka, to the west of lake Tryvann, the most extensive Mo-mineralizations of the TGC are exposed (type 3). Here, numerous molybdenite veins, 5 mm across, transect the Grefsen syenite - Tryvann granite boundary. Commonly, fine-grained red K-feldspar forms alteration selvages 1 to 2 mm wide, marginal to the molybdenite veins which cross-cut brecciated and pyrite-disseminated zones of a fine-grained topaz-fluorite-albite-quartz rock within the Grefsen syenite.

On the regional scale, the molybdenite mineralizations of the TGC seem to be restricted to a zone within the alkali-feldspar granite, close to the alkali-feldspar quartz syenite boundary between Voksenåsen and Wyllerløypa. However, molybdenite and pyrite occur locally disseminated within a fine-grained scapolite-albite-quartz rock as well as within the unaltered granite (type 4) in the Skådalen granite body.

The sulphide mineralizations of type (5) are restricted to the albitized and propylitized parts of the ring-dyke complex, as mentioned earlier, in the southern part of the Bærum cauldron. The mineralizations and associated alterations were briefly mentioned by Sæther (1945). The most prominent example of this type occurs at Østerås (Fig.3) where the ring-dyke cuts the Silurian Pentamerus limestone (Rytteråker Formation, Et.7a-b) (Naterstad et al.1990). At the contact, a clinopyroxene-andradite-bearing skarn-zone, 30 cm in thickness, is developed with a heavy impregnation of pyrite, sphalerite, galena and hematite. In the adjacent, strongly propylitized part of the ring-dyke, Mo-bearing scheelite occurs as scattered anhedral grains, 0.2-0.5 mm across. However, apart from a slight sericitization of the feldspars, no significant post-magmatic hydrothermal alteration with sulphide mineralizations has been observed within the ring-dyke complex away from the Cambro-Silurian boundary.

The age relationships between different hydrothermal stages of the TGC are difficult to distinguish in the field because of the general absence of cross-cutting relationships. However, from the present field studies and petrographical observations presented above, the following sequence of hydrothermal alteration can be inferred:

1. An early albitic alteration along (parallel) fracture zones associated with an early magnetite ± hematite ± ilmenite deposition.

2. Oxidation of magnetite to hematite (martitization and general grain boundary replacement) and of ilmenite to rutile ± hematite (replacement).

3. Sulphide mineralization (pyrite ± minor molybdenite and accessory chalcopyrite ± pyrrhotite) associated with vein-quartz deposition along the established fracture zones.

4. A late molybdenite mineralization event, locally associated with a limited potassic alteration on a limited scale.

The local replacement of albite by scapolite (Skådalen) and the introduction of topaz and fluorite in the quartz-albite veins at Ringeriks-flaka may have occurred at stage 3 or later, but their relationship to the ore-forming events is not clear.

Albitization and scapolitization have also affected the contact-metasomatic, skarn-hosted oxide- and sulphide ore deposits located at the border of the Cambro-Silurian limestones and the Oslo Graben plutons (Fig.3). Albitized skarns were already recognized by Goldschmidt (1911), who described them as contact-pneumatolytic alteration products which were formed later than the formation of the iron-rich andradite-skarns.

## Tectonic relationships

The fracture pattern of the TGC and adjacent rocks shows that the hydrothermal alterations and associated ore mineralizations are confined to the following three main fracture sets intersecting the TGC (Fig.15):

1. A regional set of N-S-trending fractures which also controls the younger diabase dykes of the area (Sæther 1947).

2. A regional NNW-SSE-striking joint and fault set that comprises the Langlia fault to the northeast of the Bærum cauldron as well as a fault zone running from the lake Sognsvatn along lake St.Åklungen to the lake Skjærsjøen (Figs.2 & 3).

3. Two interfering 'cone-in-cone' concentric joint sets with foci to the south of the TGC, intersecting the Bærum Cauldron boundary.

On a local scale the straight boundaries of the plutons of the TGC in general follow the trends of the prominent major fracture sets of the region (e.g. the N-S and NNW-SSE trends), which suggests that the emplacement of the TGC has been partly controlled by older tectonic lineaments in the adjacent syenitic plutons. These features are most prominent in the Skådalen granite body with its complex angular boundaries defined by at least two major fracture trends (NNW-SSE and NE-SW). In the late- and post-magmatic stages of the TGC, these fracture zones have been reactivated and mineralized. This may have happened contemporaneously with the formation of the late, concentric joint sets which show very little or no displacement. In this respect there seems to be a close relationship between the emplacement of the TGC, the fracture pattern, and the zones of alteration and mineralization of the complex.

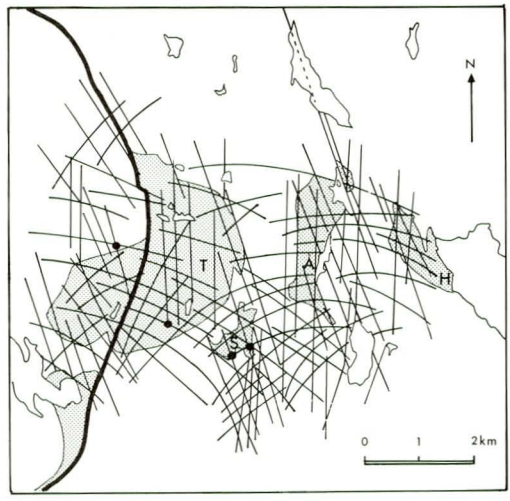


Fig. 15: Joint sets of the Tryvann Granite Complex (stippled) and adjacent rocks. The thick line marks the Bærum Cauldron boundary; cf.map, Fig.2. for locations. Granite bodies: T - Tryvann; S - Skådalen; Å - Åklungen; H - Hammeren. Dots: Mo-mineralizations.

## Discussion

The gravimetric investigations of the Bærum cauldron (Smithson 1961) revealed a positive gravity anomaly within the southern part of the cauldron which was ascribed to the presence of the B3 basalt sequence with a thickness of 1km. With the correction of this gravity effect, this resulted in a negative gravity anomaly of 10 mgal over this part of the cauldron with a strong negative gradient from lake Bogstadvatnet to the hill Tryvannshøgda. This anomaly was, according to Smithson (1961), in accordance with a gravimetric profile above a vertical quartz-syenitic cylinder with a diameter of 10 km and a height of 6 km, and with the upper surface about 3 km below the present surface within the cauldron. He suggested a possible relationship between this inferred pluton with the outcropping ring-dyke and the granitic complex of the Bogstad-Tryvann area,i.e. the TGC. A similar model was also proposed by Oftedahl (1978) who

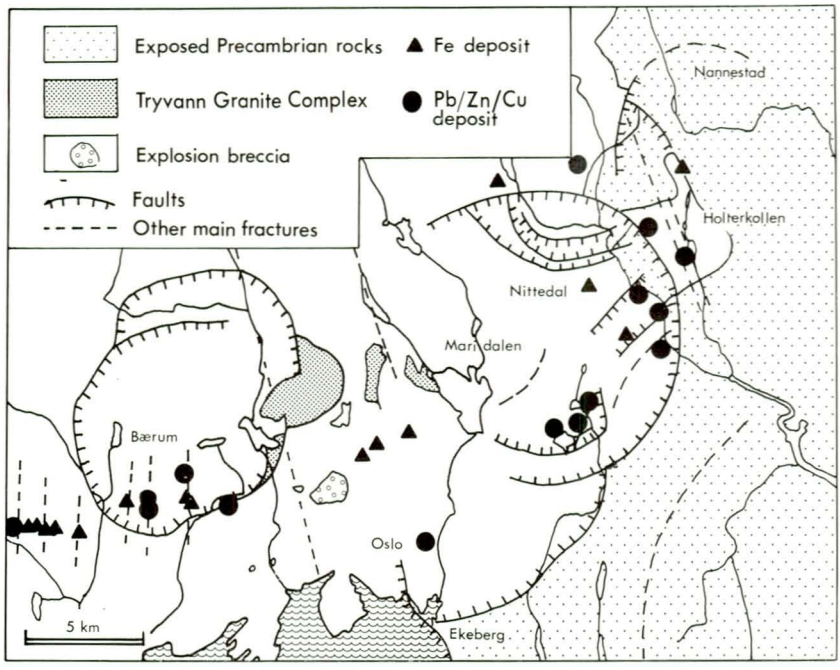


Fig. 16: Ring faults, fractures and Permian ore deposits of the Oslo district. Central Oslo Region. Modified from Naterstad (1971), Ramberg (1976) and Ihlen & Vokes (1978).

related the subsidence of the cauldron with the upward stoping of a syenitic magma which led to a collapse of the roof and the intrusion of the ring dyke along the fracture zone.

The present field observations and the mineralization patterns support the suggestions of Smithson (1961), Sæther (1962) and Petersen (1983) that the TGC neither intruded nor intersected an established Bærum cauldron boundary fault. Instead, the TGC appears to constitute an integral part of the final development of the cauldron as the ring-dyke, and the TGC apparently manifests a contemporaneous magmatic event in the initial uplift and stoping of the Cambro-Silurian metasediments and Permian magmatic rocks. Evidence for an early uplift of the Cambro-Silurian basement by an ascending pluton prior to cauldron collapse can be seen in the deflection of the NW-dipping Silurian strata and fold axial planes towards the cauldron boundaries in the southern Bærum region (Naterstad et al.1990), and the wide thermal aureole extending several kilometres away from the ring-dyke (Sæther 1945, Holtedahl & Dons 1952).

The termination of the magmatic activity is revealed in the cauldron collapse, injection of the ring-dyke and the TGC with a subsequent hydrothermal activity giving rise to the present mineralizations and alterations. A last phreatic stage may have given rise to the external explosion breccias at Jar and Øraker (Werenskiold 1918), Ullern (Dons 1952) and Holmen-Dagali (Holtedahl 1943), and also probably to similar intra-cauldron explosion breccias in the central and northern parts of the cauldron (Sæther 1962).

On a regional scale the geological pattern, expressed by the gravimetric anomalies, and the spatial metamorphic and metasomatic alteration pattern adjacent to the southern part of the Bærum cauldron reveal the existence of a (partly) hidden, ENE-WSW trending, elongated plutonic complex extending from the W.Bærum district towards the Nittedal area, linking the Bærum cauldron with the Nittedal cauldron (Naterstad 1971,1977,1978)(Fig.16). This corresponds with the inferred central volcanic axis proposed by Ramberg & Larsen (1978,p.66) between the Bærum and Nittedal districts in the Akershus Graben segment (Figs.3 & 16). This is apparently manifested by the presence of swarms of aplogranitic dykes, extending from the TGC towards lake Skjersjøen. Here, an elongated body of a (barren) rhyolitic felsite with aplogranitic margins intrudes the older alkali-feldspar syenites and extends further, along a NE-SW trend, towards Maridalen (Fig.2) and the Holterkollen granite pluton in the Nittedal area (Fig.16).

## Conclusions

The Tryvann Granite Complex (TGC) constitutes a series of alkaline quartz syenites and granites that were derived from a highly evolved granitic magma. The complex was emplaced in connection with the collapse of the Bærum Cauldron and the associated formation of a prominent ring-dyke complex. The emplacement was structurally controlled, predominantly by a system of subvertical N-S and NNW-SSW fracture sets and by the Bærum Cauldron boundary fault. The presence of miarolitic cavities within the granophyric alkalifeldspar granites suggests a rapid crystallization of a vapour-saturated magma. Post-magmatic epithermal reactions were associated with an early oxide and late sulphide deposition in different stages along secondary, healed, planar fractures within the TGC and adjacent wall-rocks. Saline fluids with high Na/K ratios and with sufficient Cl and F contents to form the secondary scapolite, topaz and fluorite assemblages were apparently involved in the formation of the present alteration parageneses enveloping the permeable channelways.

The relationship between the intraplutonic hydrothermal activity of the TGC and the formation of the several contact-metasomatic vein-type mineralizations and the different skarn-forming events in the Oslo and Bærum districts has not yet been investigated. However, a close relationship seems to exist between the stage of cauldron formation in the southern Akershus Graben, the 240-250 Ma granite plutonism of the area, and a subsequent phase of epithermal activity in the region.

*Acknowledgements*

I would like to thank B. Sundvoll and three anonymous referees for valuable comments and constructive criticism of the manuscript. I also thank T. Bjerkgård for technical support and D. Ettner and D. Roberts for improving the English language.

## References

Bjørlykke,A.,Ihlen,P.M. & Olerud,S.1990: Metallogeny and lead isotope data from the Oslo Paleorift. *Tectonophysics 178*, 109-126.

Bowden,P.1982: Magmatic evolution and mineralization in the Nigerian younger granite province. *In*: Evans, A.M. (ed.): *Metallization associated with acid magmatism.* John Wiley & Sons, Chichester 1982, 51-61.

Carmichael,I.S.E.;Turner,F.J.& Verhoogen,J.1974: *Igneous Petrology.* McGraw-Hill, New York 1974,739pp.

Dons,J.A.1952: Studies on the igneous rock complex of the Oslo region XI. Compound volcanic neck, igneous dykes, and fault zone in the Ullern - Husebyåsen area, Oslo. *Skr.Norske Vidensk.-Akad.i Oslo, I. Mat.-naturv. Kl.1952, No.2*, 96pp.

Dons,J.A.& Larsen,B.T.(eds.) 1978: The Oslo Paleorift. A review and guide to excursions. *Nor.geol.unders.337*, 199pp.

El Bouseily,A.M.& El Sokkary,A.A.1975: The relation between Rb,Ba and Sr in granitic rocks. *Chem.Geol.16*, 207-219.

Gaut,A.1981: Field relations and petrography of the biotite granites of the Oslo Region. *Nor.geol.unders.367*, 39-64.

Geyti,A.& Schönwandt,H.K.1979: Bordvika - a possible porphyry molybdenum occurrence within the Oslo Rift, Norway. *Econ.Geol.74*, 1211- 1220.

Goldschmidt,V.M.1911: Die Kontaktmetamorphose im Kristianiagebiet. *Vidensk.Selsk.Skr.I.Mat.-Naturv.Kl.1911, No.1*, 483pp.

Holtedahl,O.1943: Studies on the igneous rock complex of the Oslo region I. Some structural features of the district near Oslo. *Skr.Norske Vidensk.-Akad.i Oslo, I. Mat.-naturv.Kl.1943, No.2*, 71pp.

Holtedahl,O.& Dons,J.A.1952: *Geologisk kart over Oslo og Omegn.* Det Norske Videnskaps-Akademi i Oslo 1952.

Huseby,S.1971: Studies on the igneous rock complex of the Oslo region XXII. Permian igneous dikes in the southern part of the Bærum Cauldron. *Skr.Norske Vidensk.-Akad.i Oslo, I. Mat.-naturv.Kl.,Ny serie No.30*, 3-16.

Ihlen,P.M.1978: Ore deposits in the north-eastern part of the Oslo region and in the adjacent Precambrian areas. *In:* Neumann,E.-R.& Ramberg, I.B.(eds.): *Petrology and geochemistry of continental rifts.* D.Reidel Publ. Comp.,Dordrecht 1978,277-286.

Ihlen,P.M.1986: The geological evolution and metallogeny of the Oslo Paleorift. *Sver.Geol.Unders. Ser.Ca 59*, 6-17.

Ihlen,P.M.& Vokes,F.M. 1978: Metallogeny. *In:* Dons,J.A. & Larsen,B.T. (eds.): The Oslo Paleorift. *Nor.geol.unders. 337*, 75-90.

Ihlen,P.M.,Trønnes,R.& Vokes,F M.1982: Mineralization, wall-rock alteration and zonation of ore deposits associated with the Drammen Granite in the Oslo region, Norway. *In:* Evans,A.M.(ed.): *Metallization associated with acid magmatism.* John Wiley & Sons 1982,111-136

Kinnaird,J.A.1985: Hydrothermal alteration and mineralization of the alkaline anorogenic ring complexes of Nigeria. *J.Afr.Earth Sci.3*, 229-251.

Kinnaird,J.A.,Batchelor,R.A.,Whitley,J.E.& MacKenzie,A.B. 1985: Geochemistry, mineralization and hydrothermal alteration of the Nigerian high heat producing granites. *In: High heat production (HHP) granites, hydrothermal circulation and ore genesis.* Proc.Inst.Min.Metall.,London 1985,169-195.

Larsen,B.T.& Sundvoll,B.1982: Episodisk utvikling av Oslo riften - resultater fra nyere radiometriske dateringer. (Abstr.) *Geologynytt 17*, 34.

Manning,D.A.C.1981: The effect of fluorine on liquidus phase relationships in the system Qz-Ab-Or with excess water at 1kb. *Contrib. Mineral. Petrol. 76*, 206-215.

Naterstad,J.1971: Nittedal Cauldron. *Nytt fra Oslofeltgruppen 1*, 29-41.

Naterstad,J.1977: Alnsjø-feltet. *In:* Dons,J.A.(ed.): *Geologisk fører for Oslo-trakten.* Universitetsforlaget,1977,145-150.

Naterstad,J.1978: Nittedal Cauldron (Alnsjøen area). *Nor. geol.unders.337*, 99-104.

Naterstad,J.& Dons,J.A.1978: Introductory field trip in the central part of the Oslo Rift (the surroundings of Oslo). *Nor.geol.unders.337*, 93-97.

Naterstad,J.; Bockelie,J.F.; Bockelie,T.; Graversen,O.; Hjelmeland,H.; Larsen,B.T.& Nilsen,O.1990: *ASKER 1814 I, berggrunnskart M.1:50 000.* Nor.geol.unders. 1990

Neumann,E.-R.1978: Petrology of the plutonic rocks. *In:* Dons,J.A.& Larsen, B.T.(eds.) 1978: The Oslo Paleorift. A review and guide to excursions. *Nor.geol.unders.337*, 93-97.

Neumann,E.-R.1980: Petrogenesis of the Oslo Region larvikites and associated rocks. *J.Petrol.21*, 498-531.

Neumann,E.-R.1988: Isotopic and petrological relations of the crust and upper mantle under the Oslo Graben, Southeast Norway. *Nor.geol. unders. Spec. Publ.3*, 7-13.

Neumann,E.-R.,Tilton,G.R.& Tuen,E.1988: Sr, Nd and Pb isotope geochemistry of the Oslo Rift igneous province, southern Norway. *Geochim.Cosmochim.Acta 52*, 1997-2007.

Neumann,E.-R.(ed.) 1990: Rift zones in the continental crust of Europe - geophysical, geological and geochemical evidence: Oslo-Horn Graben. *Tectonophysics 178*, 126pp.

Neumann,E.-R.& Ramberg,I.B.(eds.) 1978: *Petrology and geochemistry of continental rifts.* D.Reidel Publ.Comp., Dordrecht 1978, 296pp.

Nilsen,O.1990: Tryvann Granittkompleks i Oslofeltet - tektonomagmatiske og epithermale aspekter. *Geonytt 17, Nr.1*, 83.

Oftedahl,C.1946: Studies on the igneous rock complex of the Oslo region VI.On akerites, felsites, and rhomb porphyries. *Skr.Norske Vidensk.- Akad.i Oslo, I. Mat.-naturv.Kl.1946, No.1*, 51pp.

Oftedahl,C.1952:Cauldron subsidences of the Oslo Region. *Proc. 18th. Int. Geol. Congr.,Great Britain 1948,Pt.13*, 205-213.

Oftedahl,C.1953: Studies on the igneous rock complex of the Oslo region XIII. The cauldrons. *Skr.Norske Vidensk.-Akad.i Oslo, I. Mat.- naturv.Kl.1953, No. 3*, 108pp.

Oftedahl,C.1957: Studies on the igneous rock complex of the Oslo region XVI. On ignimbrite and related rocks. *Skr.Norske Vidensk.-Akad.i Oslo, I. Mat.-naturv.Kl.1957, No.4*, 21pp.

Oftedahl,C.1960: Permian rocks and structures of the Oslo Region. *In:* Holtedahl,O.(ed.): Geology of Norway. *Nor. geol.unders.208*, 298- 343.

Oftedahl,C.1978: Cauldrons of the Permian Oslo Rift. *J. Volcanol. Geotherm. Res.3*, 343-371.

Oftedahl,C.1980: Geology of Norway. *Nor.geol.unders.356*, 3-114.

Pedersen,F.D.1986: An outline of the geology of the Hurdal area and the Nordli granite molybdenite deposit. *Sver.Geol.Unders.Ser.Ca 59*, 18-23.

Petersen,J.S.1983: *Porfyr Mo mineraliseringer i Tryvannskomplekset.* Unpubl. Rep., Århus Univ.1983, 17pp.

Ramberg,I.B.1976: Gravity interpretation of the Oslo Graben and associated igneous rocks. *Nor.geol.unders.325*, 193pp.

Ramberg,I.B.& Larsen,B.T.1978: Tectonomagmatic evolution. *In:* Dons,J.A.& Larsen,B.T.(eds.): The Oslo Paleorift. *Nor.geol.unders.337*, 55-73.

Rasmussen,E.,Neumann,E.-R.,Andersen,T.,Sundvoll,B., Fjerdingstad,V.& Stabel,A. 1988: Petrogenetic processes associated with intermediate and silicic magmatism in the Oslo rift, south-east Norway. *Mineral.Mag.365*, 293-307.

Ro,H.E.,Stuevold,L.M.,Faleide,J.I.& Myhre,A.M.1990: Skagerrak Graben - the offshore continuation of the Oslo Graben. *Tectonophysics 178*, 1- 10.

Sæther,E.1945: Studies on the igneous rock complex of the Oslo region III. The southeastern part of the Bærum-Sørkedal cauldron. *Skr.Norske Vidensk.-Akad.i Oslo, I. Mat.-naturv.Kl.1945, No.6*, 61pp.

Sæther,E.1947: Studies on the igneous rock complex of the Oslo region VIII. The dykes in the Cambro-Silurian of lowland of Bærum. *Skr.Norske Vidensk.-Akad.i Oslo, I. Mat.-naturv.Kl.1947, No.3*, 60pp.

Sæther,E.1962: Studies on the igneous rock complex of the Oslo region XVIII. General investigation of the igneous rocks in the area north of Oslo. *Skr.Norske Vidensk.-Akad.i Oslo, I. Mat.-naturv.Kl.,Ny serie No.1*, 184pp.

Schönwandt,H.K.& Petersen,J.S.1983: Continental rifting and porphyry-molybdenum occurrences in the Oslo Region, Norway. *Tectonophysics 94*, 609-631.

Smithson,S.B.1961: A regional gravity study over the Permian Bærum cauldron of the Oslo region. *Nor.Geol.Tidsskr.41*, 211-222.

Sundvoll,B.1978: Rb/Sr-relationship in the Oslo igneous rocks. *In:* Neumann,E.-R.& Ramberg,I.B.(eds.): *Petrology and geochemistry of continental rifts.* D.Reidel Publ. Comp.,Dordrecht 1978, 181-184.

Sundvoll,B.& Larsen,B.T.1990: Rb-Sr isotope systematics in the magmatic rocks of the Oslo Rift. *Nor.geol.unders. Bull.418*, 27-46.

Sundvoll,B.,Neumann,E.-R.,Larsen,B.T.& Tuen,E.1990: Age relations among Oslo Rift magmatic rocks: implications for tectonic and magmatic modelling. *Tectonophysics 178*, 67-87.

Tuttle,O.F.& Bowen,N.L.1958: Origin of granite in the light of experimental studies in the system $NaAlSi_3O_8$-$KAlSi_3O_8$-$SiO_2$-$H_2O$. *Geol. Soc. Am. Mem. 74*, 153pp.

Vokes,F.M.1973.: Metallogeny possibly related to continental breakup in southwest Scandinavia. *In* Tarling,D.H.& Runcorn,S.K.(eds): *Implications of continental drift to the earth sciences.Vol.1.* Academic Press, London, 573-579.

Vokes,F.M.1988: Latest Proterozoic and Phanerozoic metallogeny in Fennoscandia *Proc.7th IAGOD Symp.,Schweizerbart'sche Verlagsbuchhandlung, Stuttgart 1988*, 41-58.

Werenskiold,W.1918: Explosionsrør ved Lysaker. *Nor.Geol. Tidsskr.5*, 99-104.

*Manuscript received February 1991; final revised typescript March 1992; accepted April 1992.*